AERODYNAMICS & BLADE TECHNOLOGY II

LOAD RESPONSE AND FLOW CHARACTERISTICS UNDER DIFFERENT AMPLITUDE FLOATER MOTIONS

Néstor Ramos-García

INTRODUCTION

- Investigation carried out as part of the COREWIND project which aims to provide disruptive and cost-effective solutions for floating offshore wind technology.

- This presentation is based on the following research work:

corewind
COST REDUCTION OF
FLOATING WIND TECHNOLOGY

RESEARCH ARTICLE *

Investigation of the floating IEA Wind 15 MW RWT using vortex methods Part I: Flow regimes and wake recovery

Néstor Ramos-García[1], Stavros Kontos[2], Antonio Pegalajar-Jurado[2], Sergio González Horcas[1] and Henrik Bredmose[2]

[1] Aero- and Fluid Dynamics section
[2] Response, Aero-elasticity, Control and Hydrodynamics section
Department of Wind Energy, Building 403, Technical University of Denmark, DK-2800 Kgs. Lyngby, Denmark

RESEARCH ARTICLE **

Investigation of the floating IEA Wind 15 MW RWT using vortex methods Part II: Wake impact on downstream turbines under turbulent inflow

Néstor Ramos-García[1], Stavros Kontos[2], Antonio Pegalajar-Jurado[2], Sergio González Horcas[1] and Henrik Bredmose[2]

[1] Aero- and Fluid Dynamics section
[2] Response, Aero-elasticity, Control and Hydrodynamics section.
Department of Wind Energy, Building 403, Technical University of Denmark, DK-2800 Kgs. Lyngby, Denmark

* Accepted for publication in WE
** Under review in WE

IEA WIND 15 MW RWT MOUNTED ON THE WINDCRETE

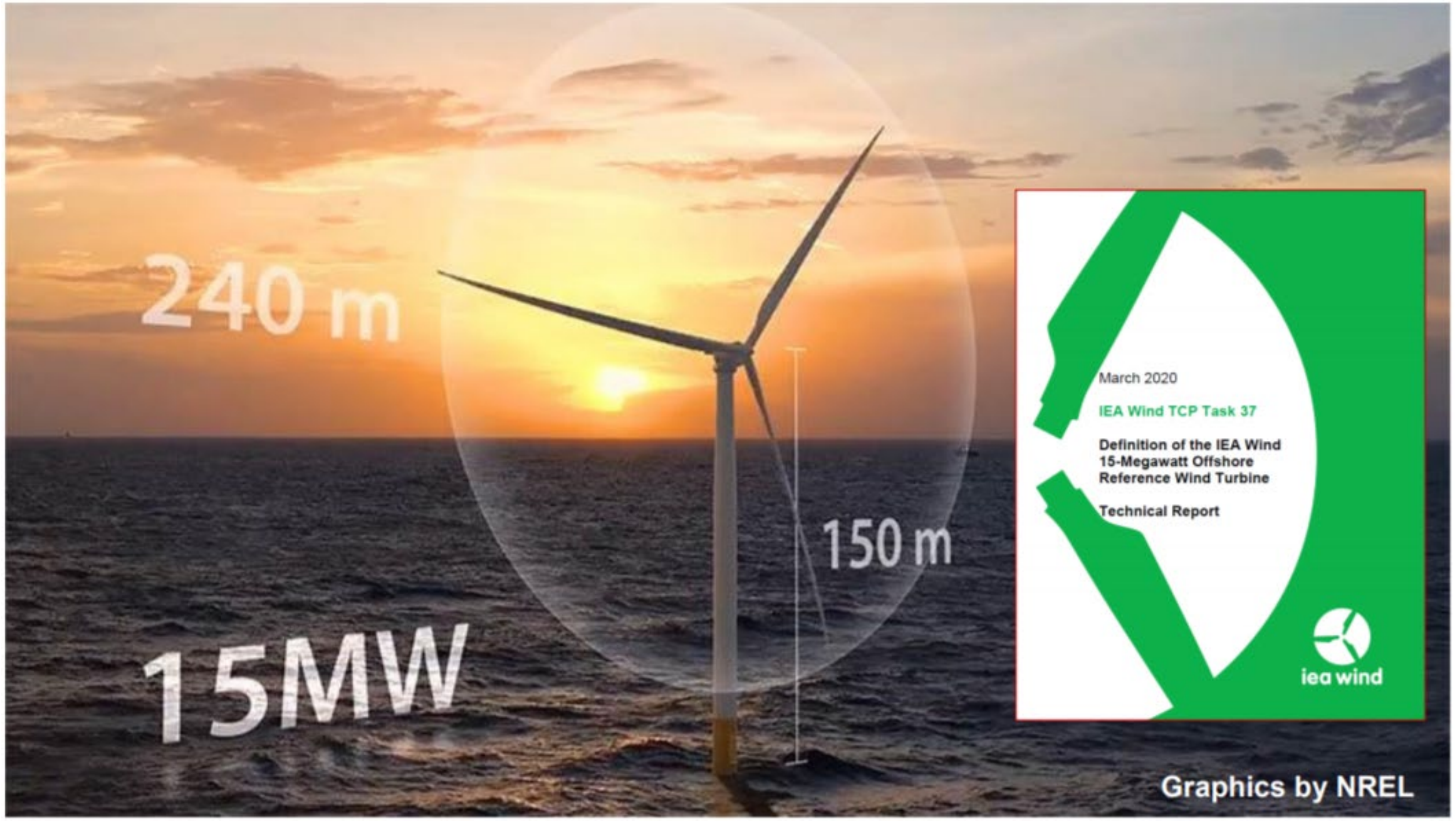

Design by NREL and DTU

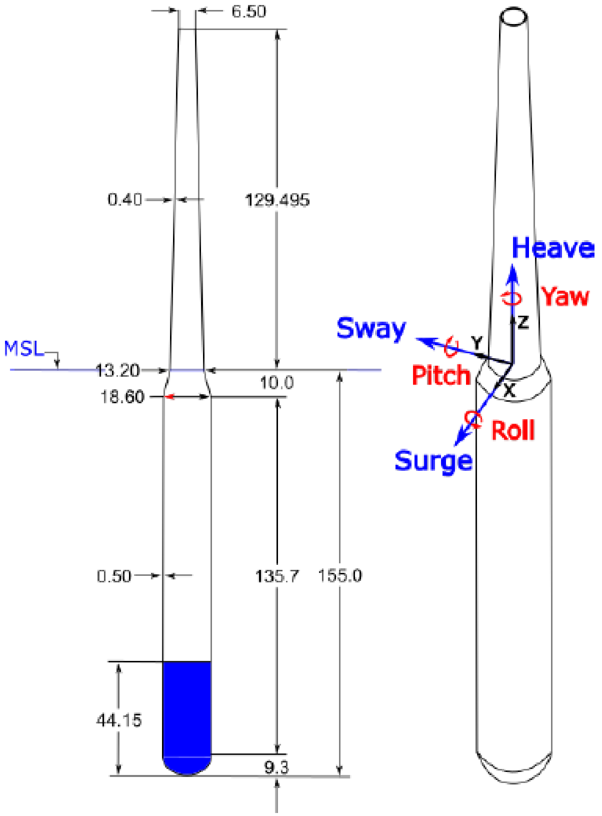

Figure 2. WindCrete Sketch with dimensions in meters. [24]

MIRAS, a multi-fidelity vortex solver

- Aerodynamic models
  - Lifting line.
  - Vortex lattice.
  - Panel method (I/VI).
- Wake/flow models
  - Filament wake(free and prescribed).
  - Hybrid wake (filaments-particles-mesh)
    - Explicit smoothing (reg.).
    - LES (Smagorinsky SGS model).
- Inflow models
  - Turbulence modelling
    - Frozen/free velocity/vorticity.
  - Wind Shear modelling
    - PVBL, P2VBL.
- Aeroelastic coupling
  - FLEX5 (direct coup. source code).
  - HAWC2 (DTU coupling tool).

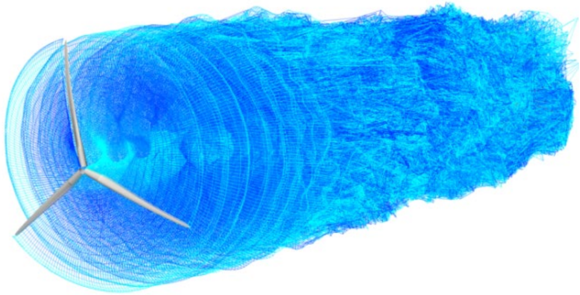

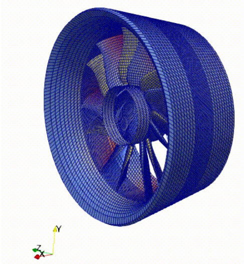

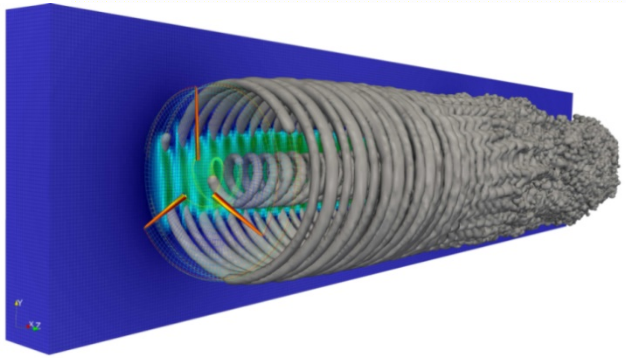

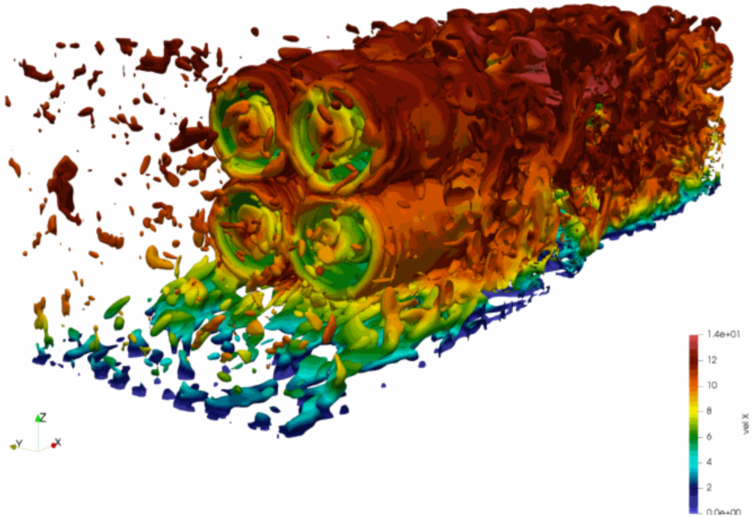

MIRAS-HAWC2 simulation setup

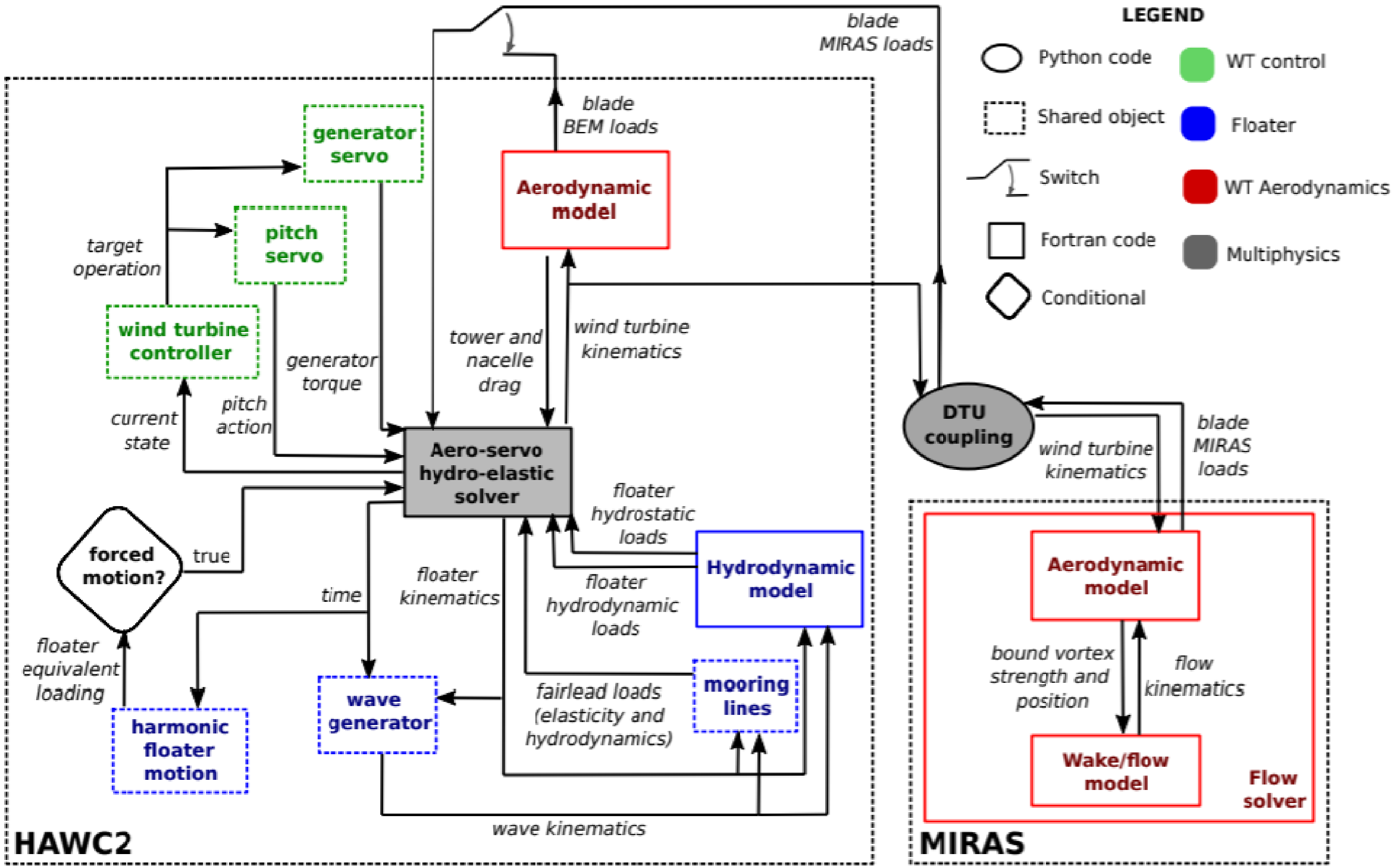

Figure 1. Sketch of the different components involved in the simulations.

IEA WIND 15 MW RWT MOUNTED ON THE WINDCRETE

Simulated cases:

- **Bottom-fixed turbine**
- Floating turbine without waves
- Floating turbine with waves

larger std predicted by LL in the tip region due to the ground modelling

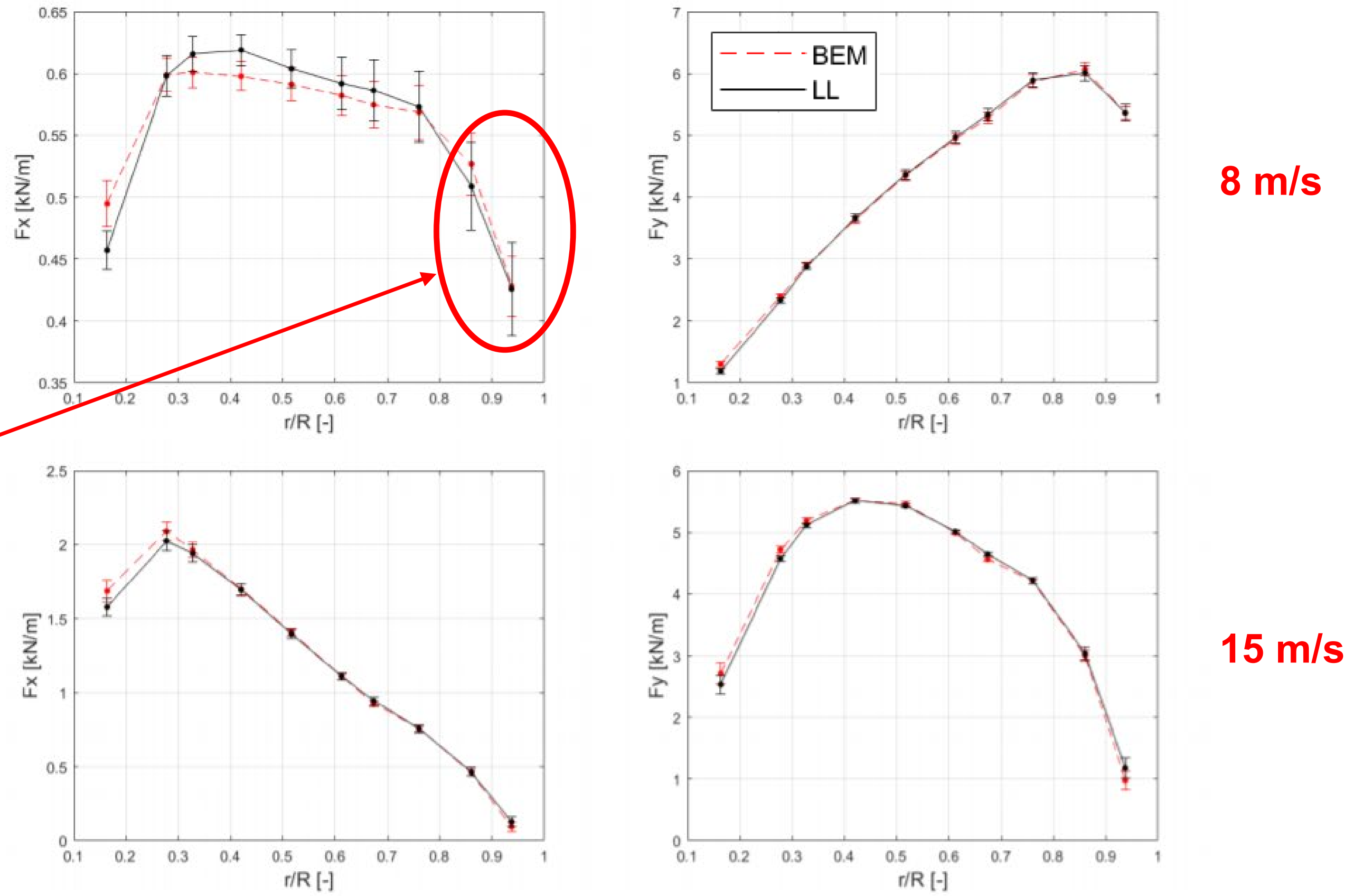

Figure 3. Mean and standard deviation of the in-plane and out-of-plane blade 1 forces for the bottom-fixed IEA Wind 15 MW RWT. **HAWC2-BEM** in dashed red lines and **MIRAS-HAWC2** in solid black lines. (top) 8 m/s (bottom) 15 m/s.

IEA WIND 15 MW RWT MOUNTED ON THE WINDCRETE

Simulated cases:

- Bottom-fixed turbine
- **Floating turbine without waves**
- Floating turbine with waves

Slightly larger differences observed at 15 m/s

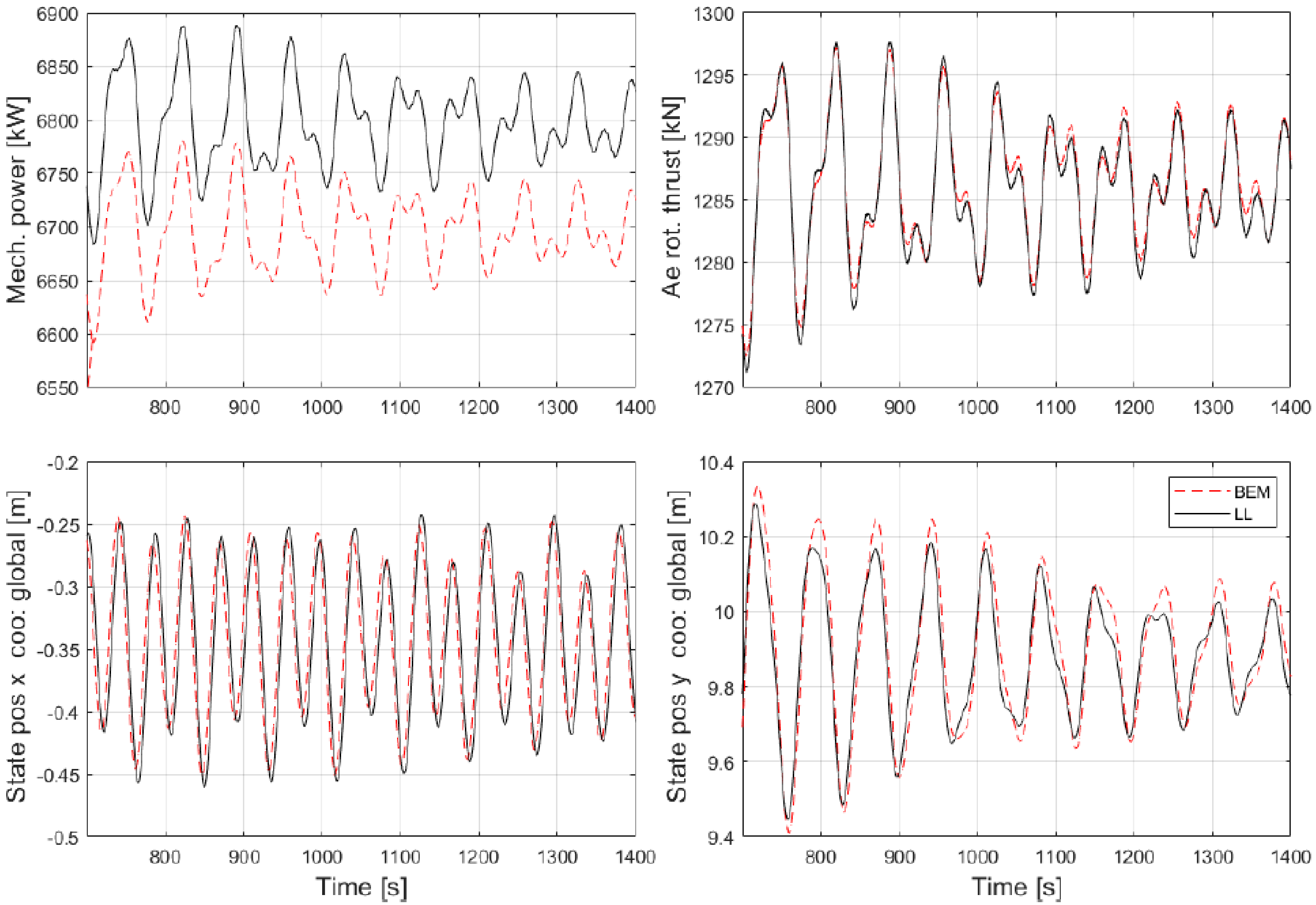

Figure 4. Floating IEA Wind 15 MW RWT mounted on the WindCrete platform without waves, comparison between **BEM** and **LL** simulations. 8 m/s wind speed.

IEA WIND 15 MW RWT MOUNTED ON THE WINDCRETE

Simulated cases:

- Bottom-fixed turbine
- Floating turbine without waves
- **Floating turbine with waves**

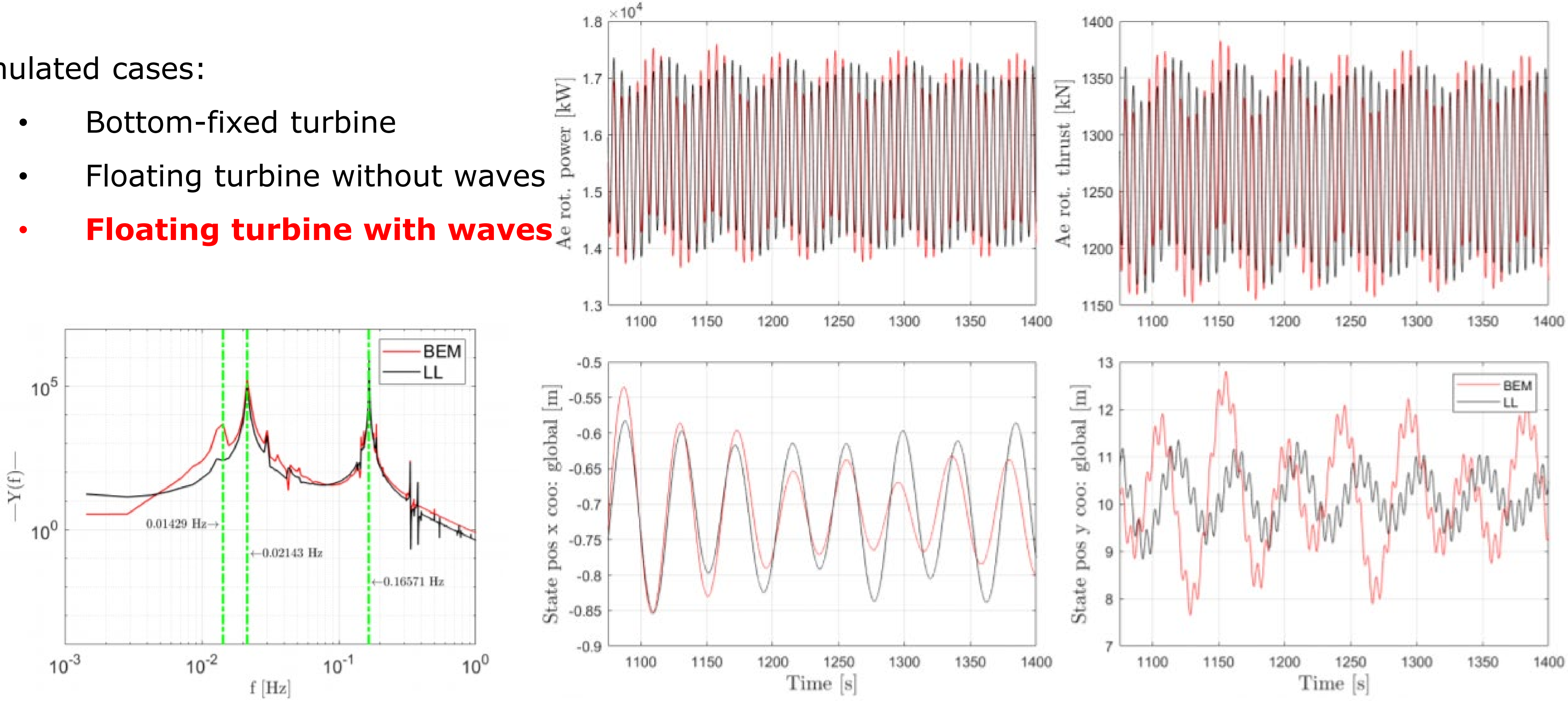

Figure 7. Floating IEA Wind 15 MW RWT mounted on the WindCrete platform and subject to regular waves with 2 m height period of 6 s. Comparison between **BEM** and **LL** simulations. 15 m/s case.

IEA WIND 15 MW RWT - WAKE DEVELOPMENT

Bottom Fixed

WindCrete Floater

Bottom Fixed

WindCrete Floater

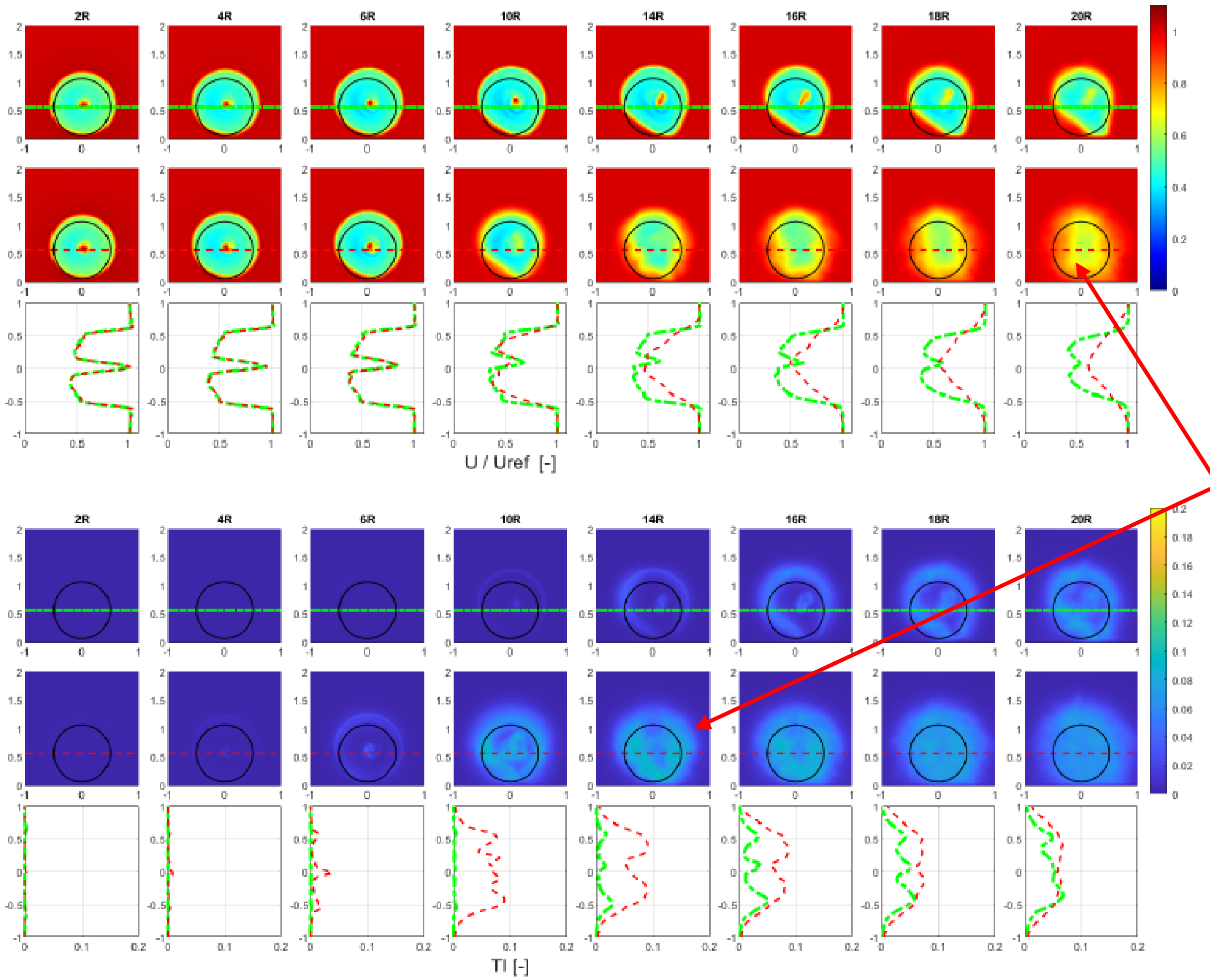

Floater motion causes a higher TI level and a faster wake recovery

Figure 9. Comparison between the wakes behind the bottom-fixed and the floating IEA Wind 15 MW RWT at different downstream distances from the rotor plane. Mean stream-wise velocity and turbulence intensity contours on multiple YZ planes downstream the rotor plane (top sub-figures) bottom-fixed case and (mid sub figures) floating case. (bottom sub-figures) profiles along the horizontal marked line at hub height.

PRESCRIBED FLOATER MOTION STUDY

PITCH

	Floater pitch frequency	Floater pitch amplitude
Frequency study	0.01419 Hz 0.02838 Hz 0.05676 Hz 0.11352 Hz	6.38 deg
Amplitude study	0.02441 Hz	3.19 deg 6.38 deg 12.7 deg

Table III. Test matrix for the prescribed harmonic pitch motion.

SURGE

	Floater surge frequency	Floater surge amplitude
Frequency study	0.01419 Hz 0.02838 Hz 0.05676 Hz 0.11352 Hz	15 m
Amplitude study	0.01419 Hz	5 m 10 m 15 m

Table IV. Test matrix for the prescribed harmonic surge motion.

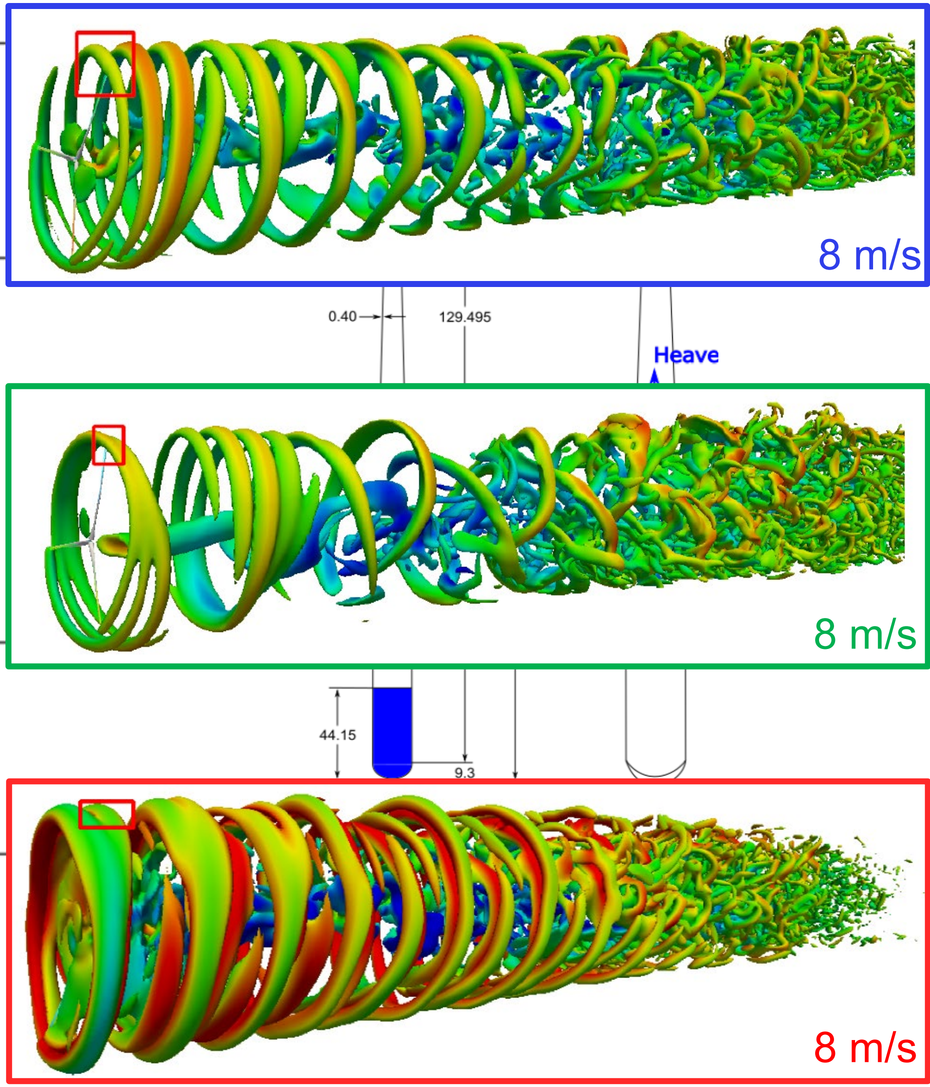

PRESCRIBED FLOATER MOTION STUDY

PITCH

	Floater pitch frequency	Floater pitch amplitude
Frequency study	0.01419 Hz 0.02838 Hz 0.05676 Hz 0.11352 Hz	6.38 deg
Amplitude study	0.02441 Hz	3.19 deg 6.38 deg 12.7 deg

Table III. Test matrix for the prescribed harmonic pitch motion.

SURGE

	Floater surge frequency	Floater surge amplitude
Frequency study	0.01419 Hz 0.02838 Hz 0.05676 Hz 0.11352 Hz	15 m
Amplitude study	0.01419 Hz	5 m 10 m 15 m

Table IV. Test matrix for the prescribed harmonic surge motion.

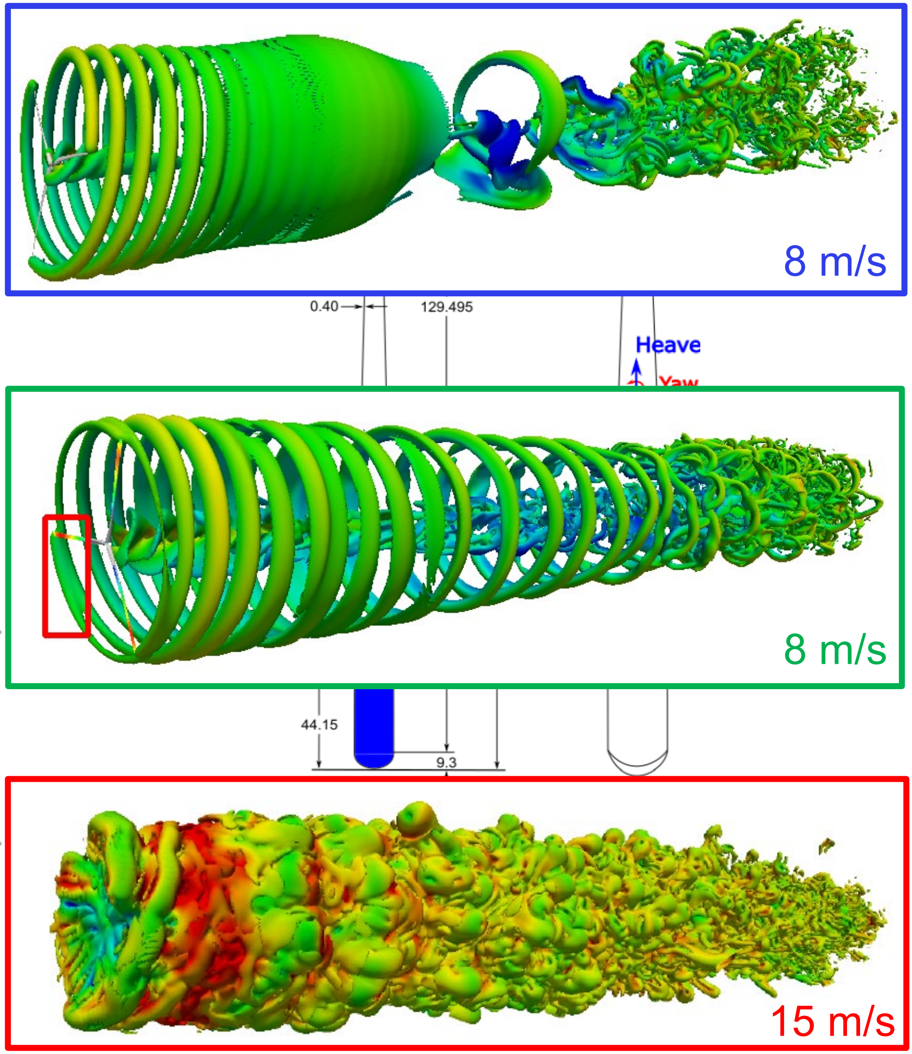

MIRAS-HAWC2 – VISUALIZATIONS

PITCH

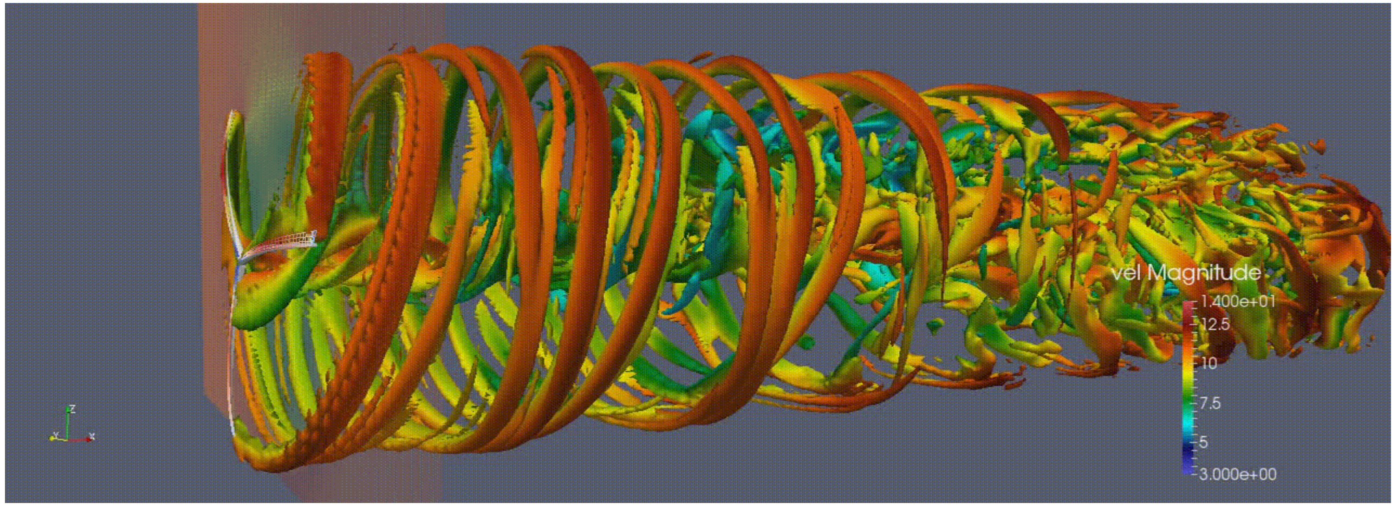

SURGE

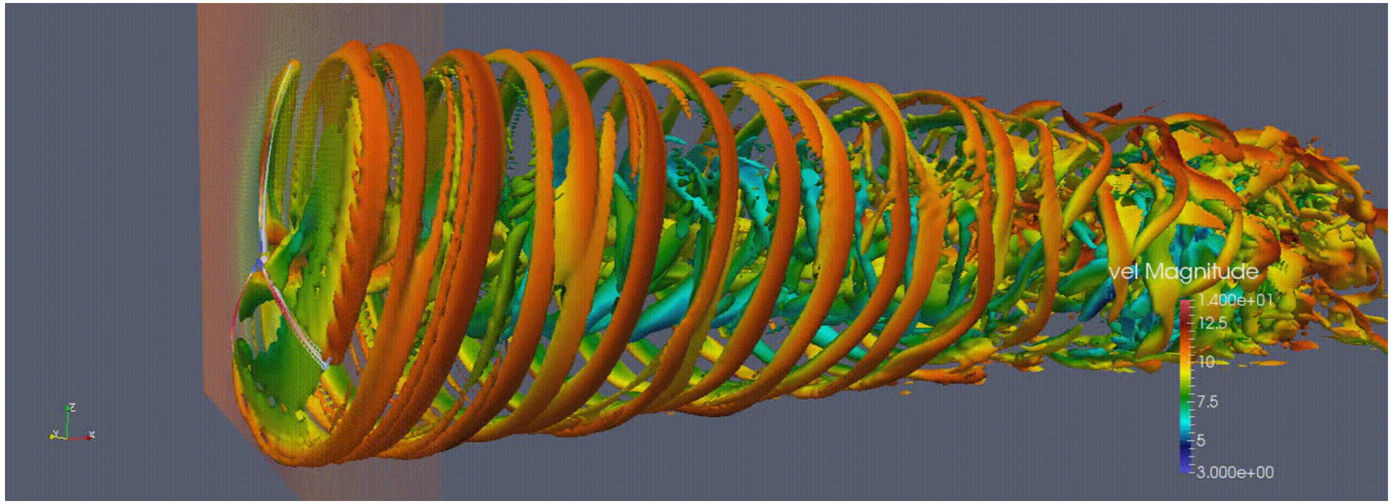

PRESCRIBED PITCH, FREQ. STUDY

8 m/s, amplitude of 6.38 degrees and different f.

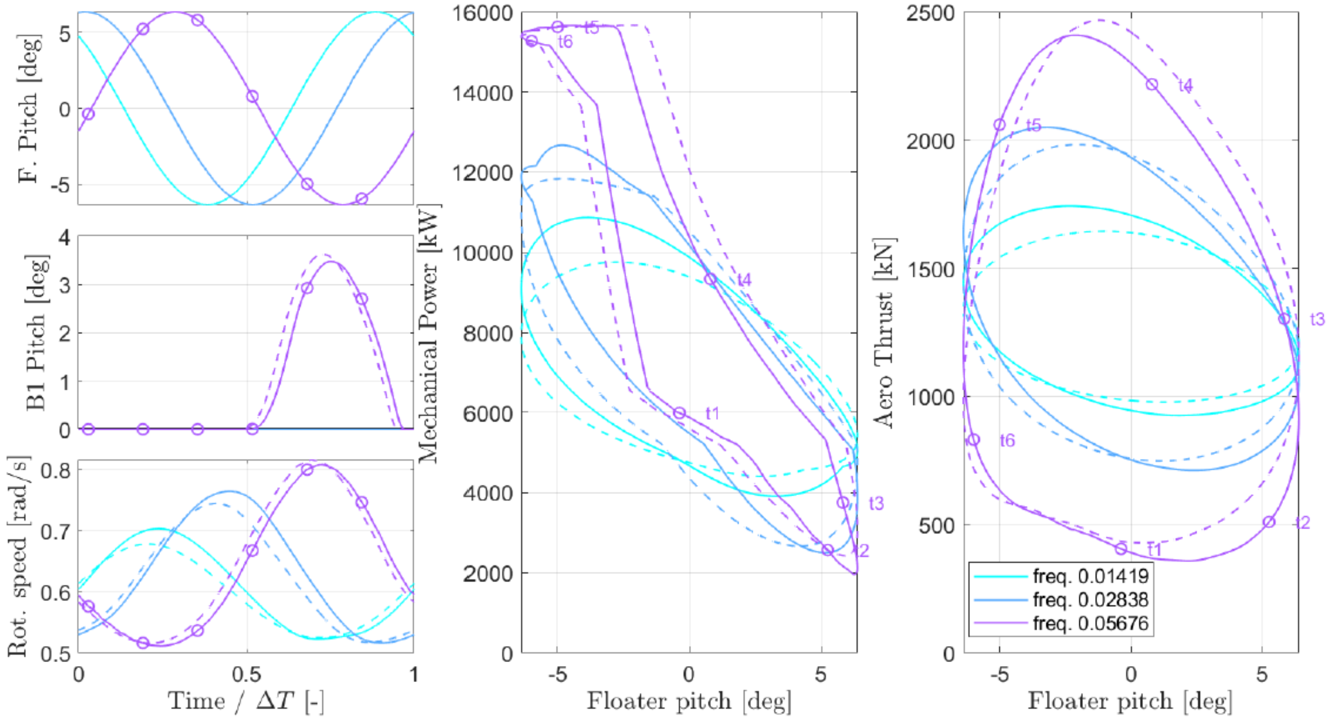

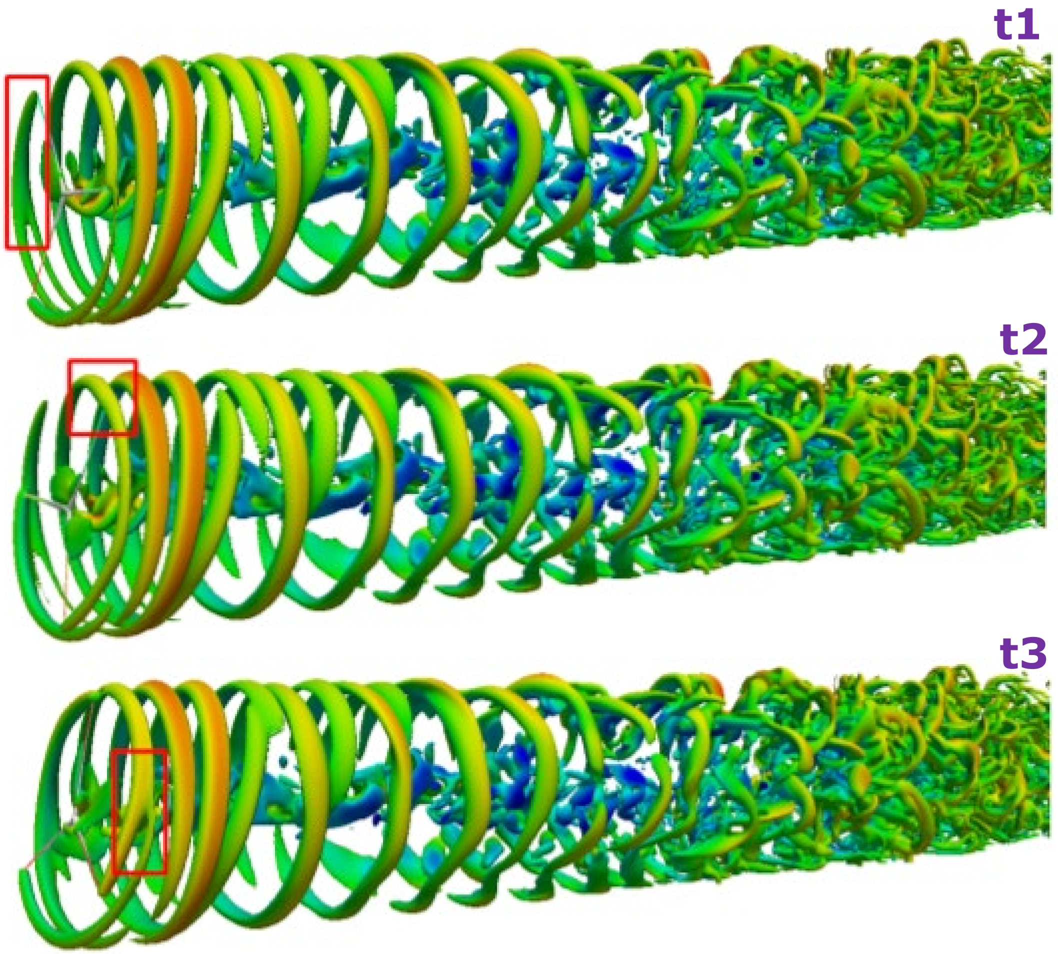

Aerodynamic quantities for the last cycle of a prescribed pitching motion of the floater with an amplitude of 6.38 degrees and different frequencies. Wind speed of 8 m/s. Solid lines represent **MIRAS-HAWC2** simulations while dashed lines represent **HAWC2-BEM**.

PRESCRIBED SURGE, WAKE

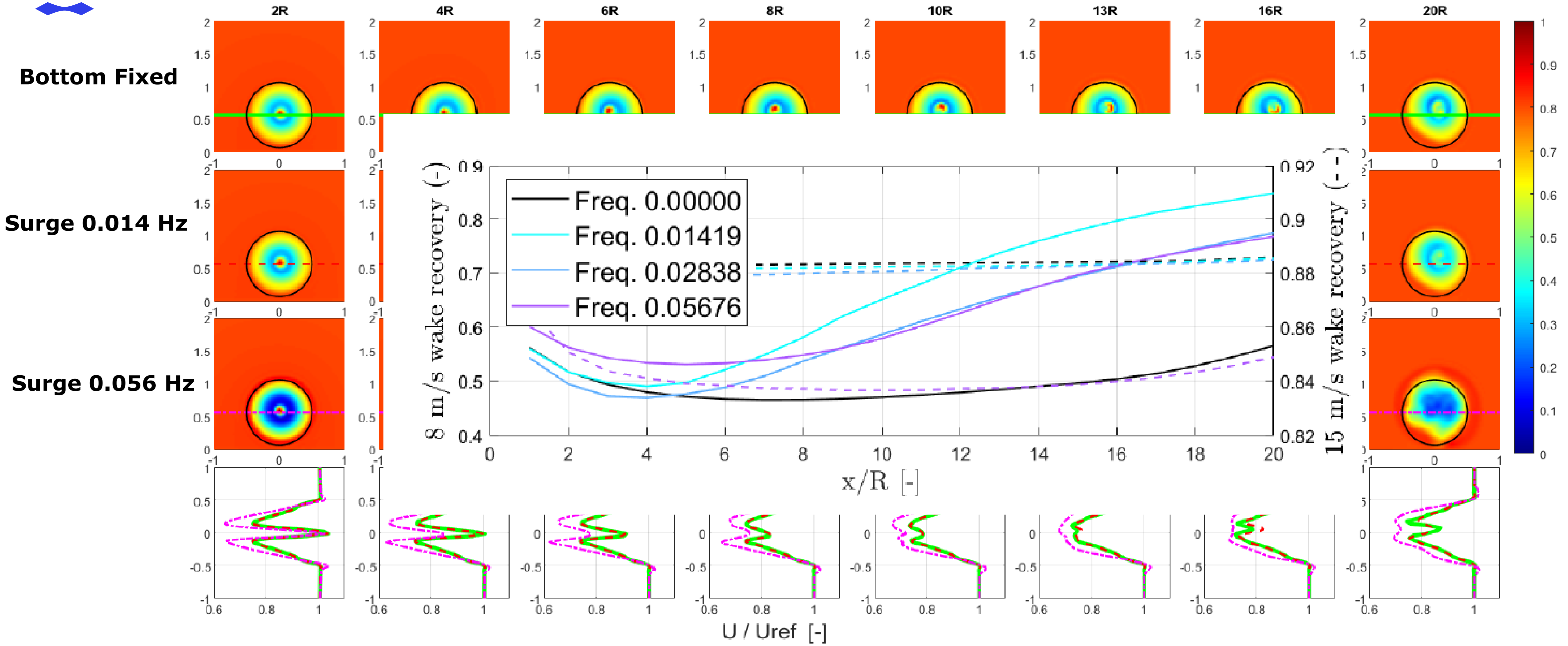

Figure 44. Mean stream-wise velocity for different surge cases at a wind speed of 15 m/s (top contours) no floater motion, (mid contours) floater harmonic surge motion of 15 m with a frequency of 0.01419 Hz and (bottom contours) floater harmonic surge motion with amplitude of 15 m and a frequency of 0.05676 Hz.

RESPONSE OF DOWNSTREAM TURBINES (2)

LAMINAR INFLOW

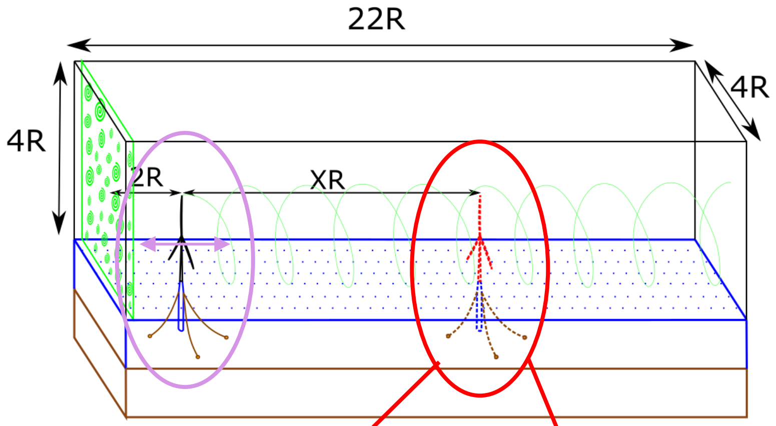

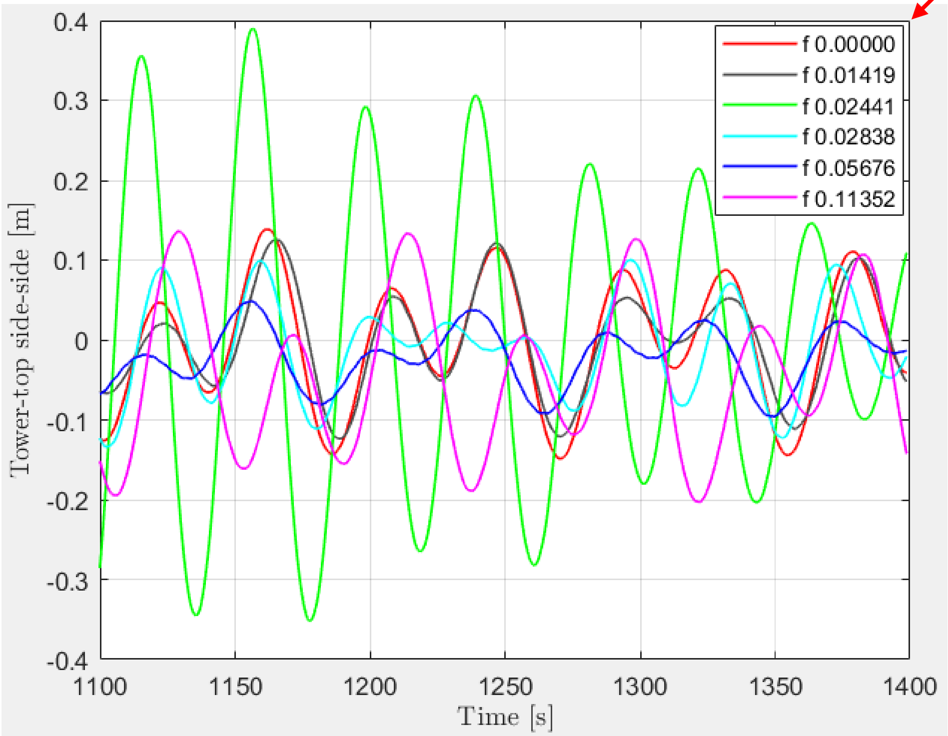

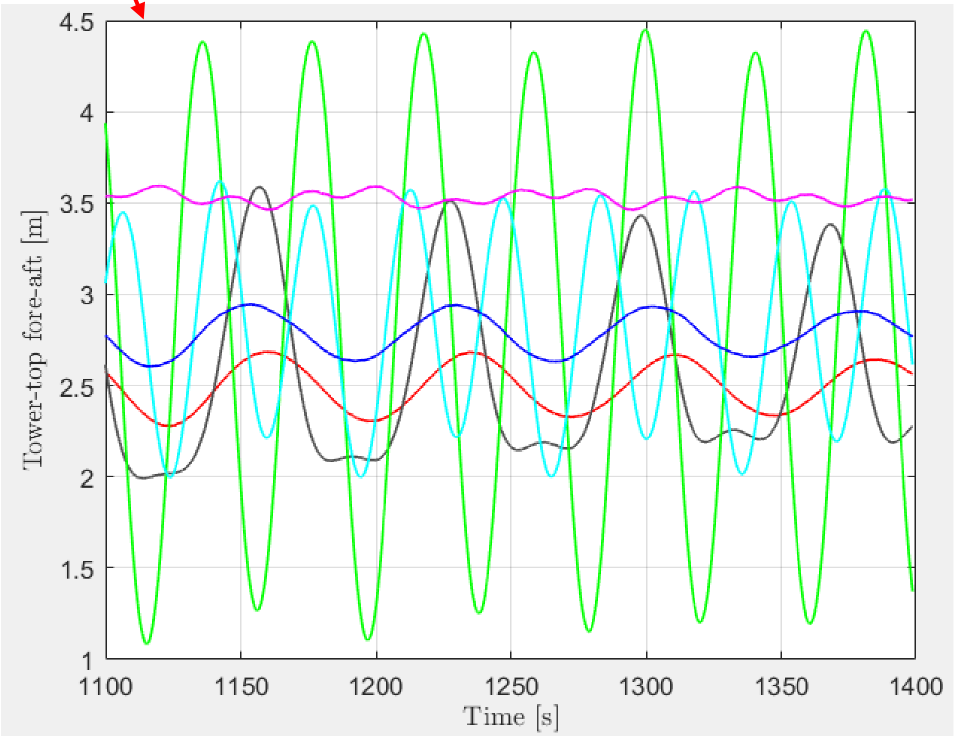

RESPONSE OF DOWNSTREAM TURBINES (5)

INFLOW TI 7 %

ALL WTs ARE FREE FLOATING

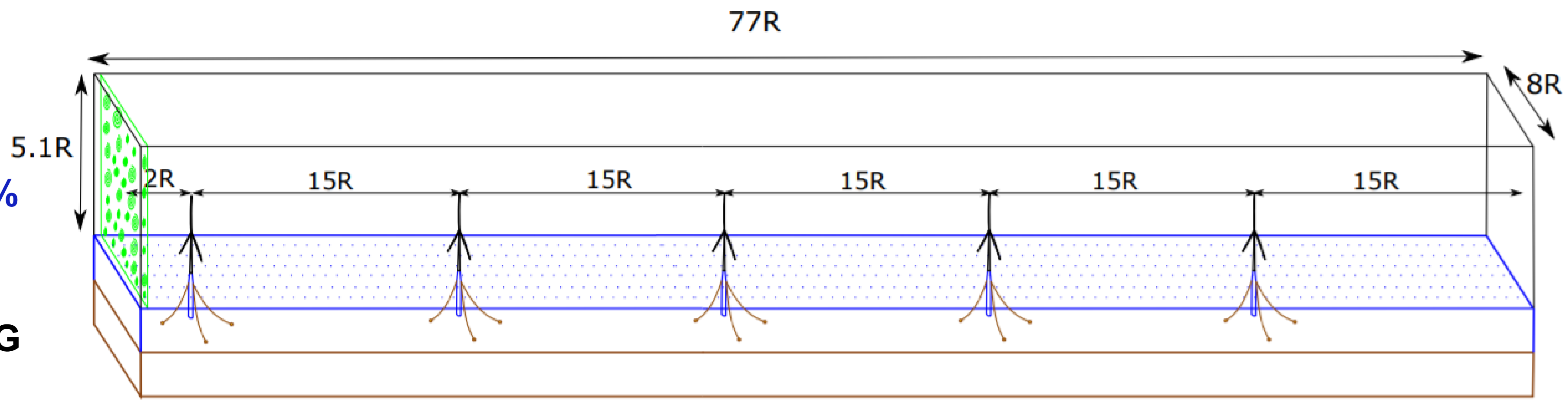

Sketch of a **MIRAS-HAWC2 farm** simulation with five floating wind turbines in a row.

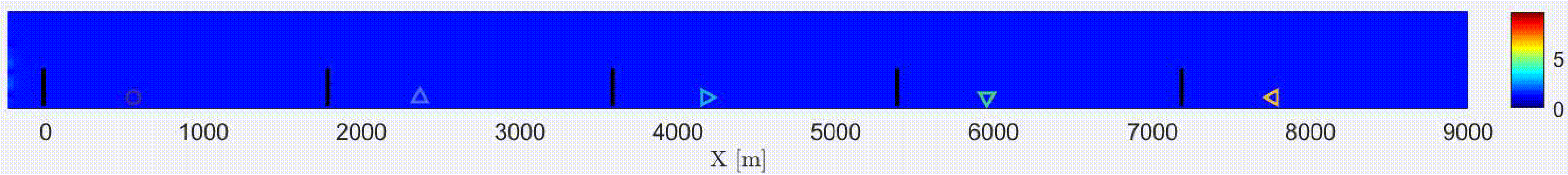

MIRAS-HAWC2 farm simulation with five floating wind turbines in a row.

RESPONSE OF DOWNSTREAM TURBINES (5)

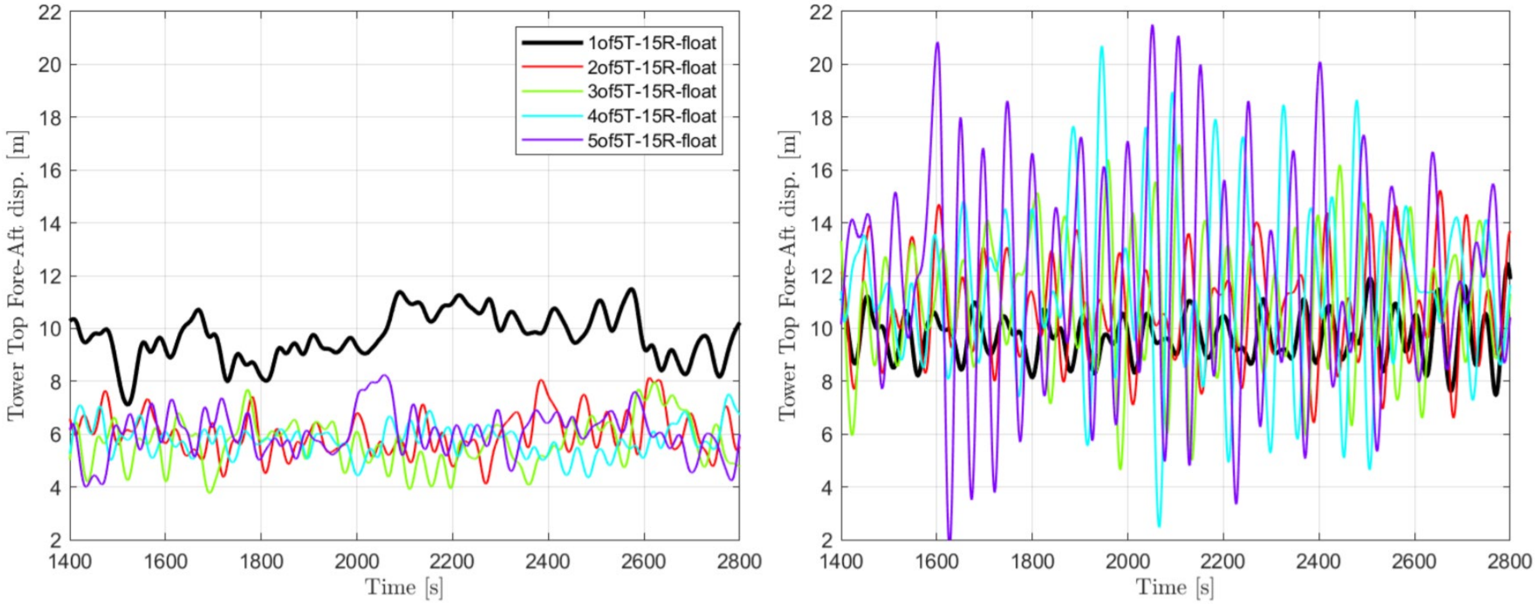

Time signal of the tower top fore-aft displacement for wind speeds of (left) 8 and (right) 15 m/s

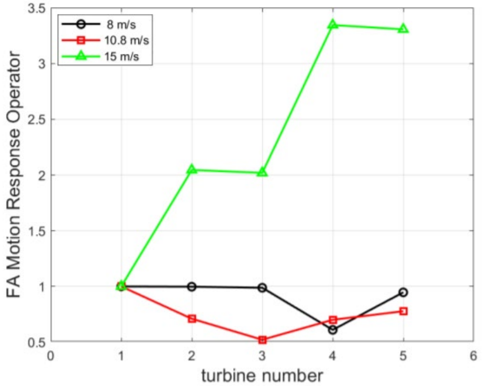

Motion response operator for the floater fore-aft displacement

CONCLUSIONS

- The **largest differences between BEM and LL** are observed **at high wind speeds**.
- The **wake of a free floating wind turbine recovers faster** in laminar inflow conditions.
- In the prescribed motion cases, the **BEM method tends to generally under-predict the rotor loading**.
- In the **pitching motion** the outer part of the blades **are more prone to local VRS than during surge**.
- In above-rated wind conditions **slow floater oscillations promote a faster wake recovery**.
- When the **upstream turbine surges at a low frequency the downstream machine draws energy at the same frequency**, creating a resonance effect.
- Farm simulations in over-rated conditions have shown that floating turbines **deep inside the farm** (WT3, WT4 and WT5) present much **larger oscillations** than more upstream located machines due to wake interaction.

DTU

RESPONSE OF DOWNSTREAM TURBINES (2)

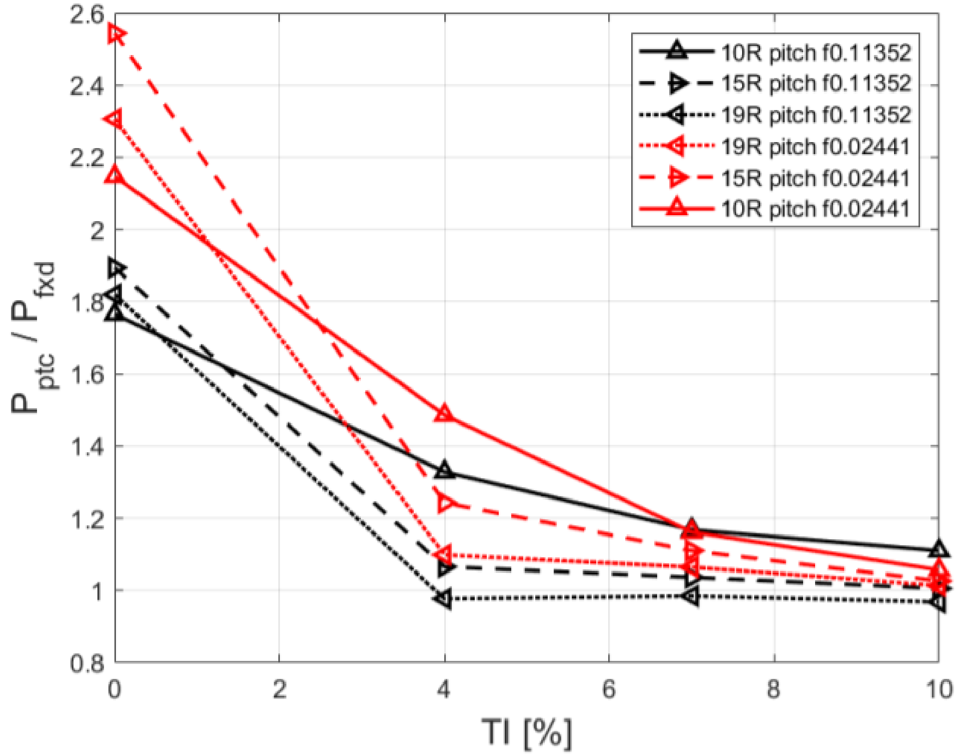

Relative mean of the power signal for the second turbine of the row with 10R, 15R and 19R spacing between turbines. Upstream turbine pitching with an amplitude of 6.38 deg and a frequency of 0.02441 Hz and 0.11352 Hz.

RESPONSE OF DOWNSTREAM TURBINES (5)

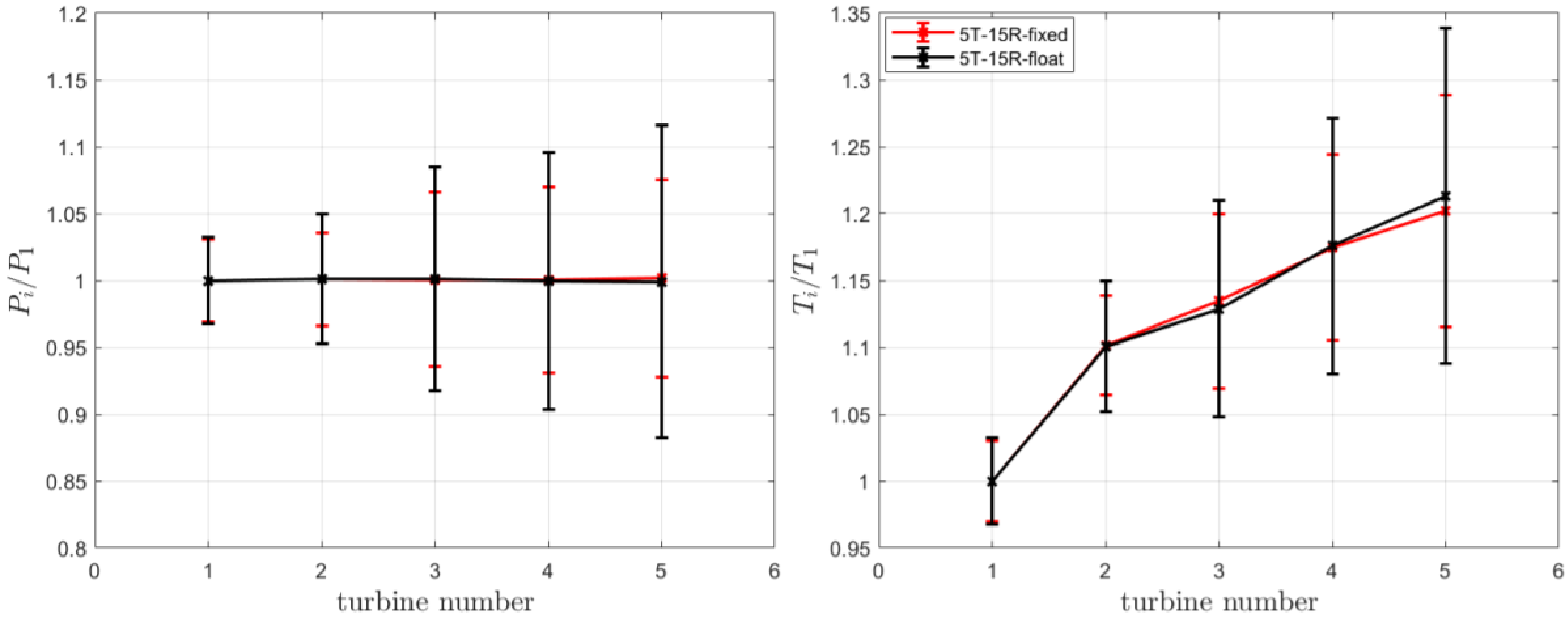

Relative mean and standard deviation of the power and thrust for the different turbines of the row in above rated wind conditions, i.e. 15 m/s.